LANDAU DAMPING IN THE LONGITUDINAL PLANE

E. Shaposhnikova, T. Argyropoulos, I. Karpov
CERN, Geneva, Switzerland

Abstract

Loss of Landau damping in the longitudinal plane can limit the performance of an accelerator and lead to particle losses via undamped bunch oscillations or to single- and multi- bunch instabilities. The threshold for loss of Landau damping for a single bunch is usually defined by comparing the position of the coherent bunch oscillation frequency with respect to the incoherent synchrotron frequency spread. Different ways of calculating this threshold are presented and compared, using the LHC as an example. Loss of Landau damping in longitudinal plane can be cured by increasing the synchrotron frequency spread, either through controlled emittance blow-up or the installation of an additional, higher-harmonic RF system.

INTRODUCTION

Landau damping is lost when the coherent bunch frequency moves outside the incoherent frequency band modified by beam-induced voltage. In longitudinal plane, Landau damping of coherent modes is achieved by synchrotron frequency spread, which can be increased by increasing bucket filling factor (minimum RF voltage for a given longitudinal emittance; limited by particle losses), increasing bunch emittance (applying controlled longitudinal emittance blow-up; limited by available RF voltage) or using a higher-harmonic RF system (in active or passive mode).

All these methods are used in CERN synchrotrons for beam stabilisation. Voltage programs through acceleration ramp are usually designed to keep buckets as full as possible while avoiding particle losses. The 4th harmonic RF system provides beam stability in the SPS together with controlled emittance blow-up, which is also necessary in LHC (see illustration in Fig. 1).

LANDAU DAMPING IN LHC

In absence of a longitudinal wide-band feedback and a higher harmonic RF system, single bunch stability in LHC should be provided by natural Landau damping thanks to the sufficient synchrotron frequency spread $\Delta\omega_s$ in the main 400 MHz RF system. The initial analysis [1] was based on Sacherer stability criterion [2], [3], which in simplified form [4] can be written as

$$\delta\omega_c < \Delta\omega_s/4, \qquad (1)$$

where $\delta\omega_c$ is the coherent dipole oscillation frequency shift and $\Delta\omega_s$ is the synchrotron frequency spread inside the bunch. It suggested that a nominal, 1 ns long, bunch will be stable at top energy of 7 TeV up to intensity of 2.4×10^{11} protons per bunch (p/b) in an RF voltage V of 16 MV, assuming an inductive impedance $\mathrm{Im}Z/n = 0.28$ Ohm. With

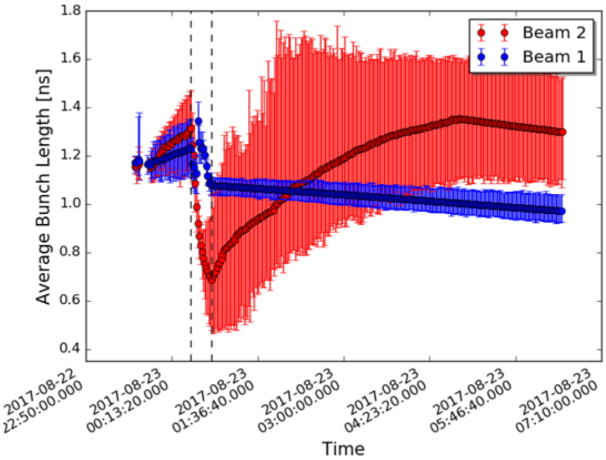

Figure 1: Measured average bunch length evolution during LHC acceleration ramp for Beam 1 with controlled emittance blow-up applied (blue line) and Beam 2 without it (red line). Continuous reduction of the bunch length in Beam 2 during the ramp (marked by the two vertical dotted lines). The stability threshold was reached and many bunches became unstable, indicated by the large bunch length spread.

a nominal bunch intensity of 1.0×10^{11} p/b, the stability margin seemed to be sufficient and wide-band feedback was not planned for LHC [5].

To avoid loss of Landau damping (LLD) during acceleration ramp, the longitudinal emittance should be increased with beam energy as $\propto E_s^{1/2}$ [6], which in operation means keeping bunch length τ constant during controlled emittance blow-up (as for Beam 1 in Fig. 1). This requirement also follows from the scaling of the LLD threshold for bunch intensity N_b, which can be derived from the criterion (1)

$$\mathrm{Im}Z/n \propto \xi = \frac{\tau^5 V}{N_b}. \qquad (2)$$

It was noticed from the start of the LHC operation that nominal bunch parameters are at the limit of longitudinal stability due to LLD. Indeed, undamped injection phase oscillations continued not only during the long flat bottom, but even survived the acceleration ramp with controlled emittance blow-up. At the top energy, a lower single-bunch stability threshold of 2×10^{11} p/b was found in measurements for a bunch length of 1 ns and low-frequency LHC impedance $\mathrm{Im}Z/n$ of 0.09 Ohm, three times smaller than the previously assumed (with safety margins) 0.28 Ohm.

Macro-particle simulations [7], performed using the code BLonD [8] and the existing LHC impedance model [9], shown in Fig. 2, agree well with measurements. Note that the simulations using constant impedance $\mathrm{Im}Z/n$ =

0.09 Ohm gave similar results to those performed with the full impedance model.

In longitudinal phase-space, bunches can be presented by a binomial particle distribution

$$\mathcal{F}(\mathcal{E}) = \mathcal{F}_0 \left(1 - \frac{\mathcal{E}}{\mathcal{E}_{\max}}\right)^{\mu}. \quad (3)$$

Here $\mathcal{E}$ is the energy of synchrotron oscillations $\mathcal{E} = \dot{\phi}^2/(2\omega_{s0}^2) + U(\phi)/(V\cos\phi_s)$ and $\mathcal{E}_{max}$ its maximum value inside the bunch; ω_{s0} is the frequency of linear synchrotron oscillations in a single RF system, $U(\phi)$ is the RF potential and ϕ_s is the synchronous phase.

In the LHC, $\mu = 2.0$ is giving a good fit to the measured bunch line density, which for short bunches in a single RF system can be presented in a simple form

$$\lambda(\phi) = \lambda_0\,(1 - \phi^2/\phi_{\max}^2)^{\mu+1/2}, \quad (4)$$

with normalisation $\int \lambda(\phi)d\phi = 1$. Here $\phi_{max} = h\omega_0\tau/2$, h is the harmonic number, τ the bunch length and $\omega_0 = 2\pi f_0$ is the revolution frequency.

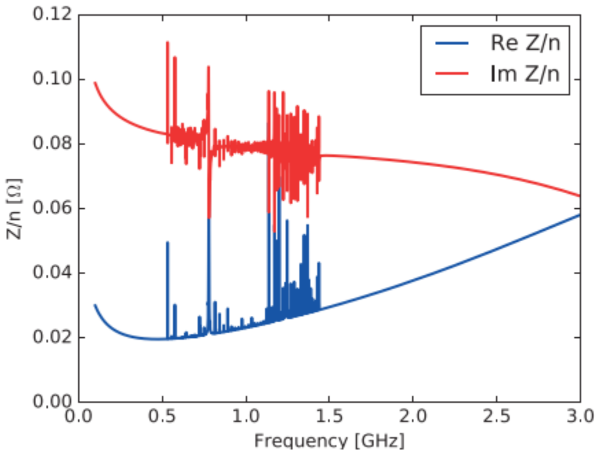

Figure 2: Longitudinal impedance model of LHC [9].

Beam measurements during acceleration ramp, at injection and top energies, as well as with various RF voltages have confirmed the expected scaling of the LLD threshold with beam energy, voltage and bunch length (in relatively small available range) giving for ξ from Eq. (2) a value of $(5.0 \pm 0.5) \cdot 10^{-5}$ [ns^{5}V], see Ref. [7] for more details.

However, the comparison of absolute threshold values indicates that the criterion (1) used for the prediction of the LLD threshold underestimates it by more than a factor 3. Since this simplified criterion is often used for design of future accelerators assuming constant ImZ/n in absence of the detailed impedance model, it is worthwhile to try and understand the reasons for the observed discrepancy.

SACHERER STABILITY DIAGRAMS

The large difference between measurements in LHC and predictions based on Sacherer criterion cannot be attributed to any “missing“ contribution in the LHC impedance model due to a good agreement between measurements and simulations. Another possible explanation could be that Eq. (1) is a simplified version of more accurate criterion which can be obtained from the Sacherer dispersion relation for a specific stationary particle distribution $F(\mathcal{E})$ [3]

$$1 = \frac{\delta\omega_{c,m}}{W_m} \int_0^{\infty} \frac{\mathcal{E}^m \mathcal{F}'(\mathcal{E})}{\omega - m\omega_s(\mathcal{E})}\, d\mathcal{E}, \quad (5)$$

where

$$W_m = \int_0^{\infty} \mathcal{E}^m \mathcal{F}'(\mathcal{E})\, d\mathcal{E},$$

and $\delta\omega_{c,m}$ is the coherent synchrotron frequency shift relative to the incoherent synchrotron frequency affected by the potential well distortion. In this approach, suggested by F. Sacherer [2], the coherent frequencies $\omega_{c,m}$ are obtained as solutions of a general matrix equation for zero synchrotron frequency spread, using the notation of the effective impedance $(\mathrm{Im}Z/n)_{\mathrm{eff}}$. Stability diagrams are then obtained as some approximation for the so-called “synthetic kernel”. This corresponds to an assumption that the wake force is proportional to the longitudinal displacement of the bunch center, valid only for a rigid bunch motion.

The dispersion relation (5) leads to stability diagrams, widely used for analysis of single bunch stability and, in particular, for the loss of Landau damping (see, for example Refs. [10] - [12]). Note that this method predicts zero LLD threshold for distribution functions (3) with $\mu \le 1$ for $\eta\mathrm{Im}Z/n < 0$ (space charge above transition), where slip factor $\eta = 1/\gamma_t^2 - 1/\gamma^2$ and γ_t is the relativistic gamma at transition energy.

The widely-used expression for the LLD threshold current

$$I_{\mathrm{th}} = \frac{m+1}{m} \frac{3\pi^2}{16} \frac{Vh^3\,(f_0\tau)^5}{(\mathrm{Im}Z/n)_{\mathrm{eff}}} \left[\frac{\delta\omega_{c,m}}{\Delta\omega_s}\right]_{\mathrm{stab}} \quad (6)$$

was found for parabolic bunches with $\mu = 0.5$. From the corresponding stability diagram, for dipole mode ($m = 1$) one gets $\left[\delta\omega_{c,m}/\Delta\omega_s\right]_{\mathrm{stab}} = 2/3$ (e.g. Ref. [12]). To obtain the criterion (1), the stability limit for $\mu = 2$ ("smooth distribution") is replaced by a semi-circle with radius $\delta\omega_c/\Delta\omega_s = 0.25$. Analytical solutions for $\omega_{c,m}$ have been found for other particle distributions (Gaussian and binomial (3) with $\mu = 0, 1$) [2]. However, analytical calculations become more involved due to the necessity to include the incoherent frequency shift.

HOFMANN-PEDERSEN APPROACH

Another possible method to evaluate the LLD threshold is based on direct comparison of the coherent oscillation frequency ω_c with the incoherent frequency band $\Delta\omega_s$ for a constant inductive impedance ImZ/n. Self-consistent analytical solutions for $\delta\omega_c$ and $\Delta\omega_s$ have been found for the specific particle distribution with a local elliptic energy distribution in longitudinal phase space [13], which corresponds to so called “parabolic” line density with $\mu = 0.5$ in Eq. (3). Only the case of $\eta\mathrm{Im}Z/n > 0$ was considered, assuming a rigid bunch motion.

The coherent frequency of rigid dipole motion does not depend on bunch intensity (see also Fig. 3) and in a single RF system can be found for any bunch profile from the relation [14]

$$\omega_c^2 = \omega_{s0}^2 \int \lambda(\phi) \cos\phi \, d\phi. \qquad (7)$$

Contrary to the Sacherer stability diagrams, the spread $\Delta\omega_s$ is taken into account in calculation of ω_c, giving non-zero threshold also for the case $\eta \mathrm{Im}Z/n < 0$, which can be evaluated in similar way. The results for LHC are shown in Fig. 3.

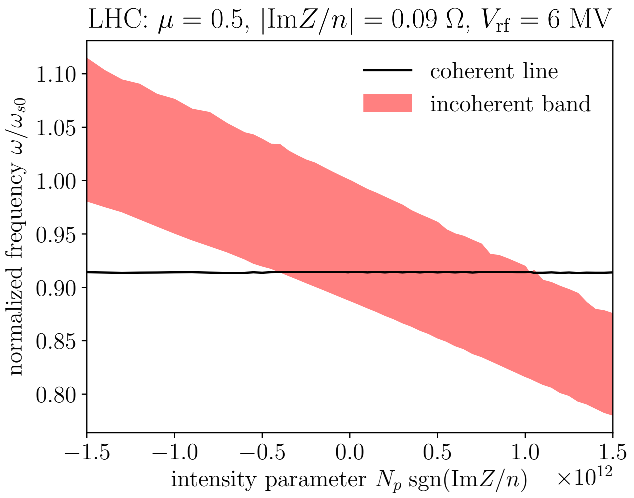

Figure 3: Coherent frequency (solid black line) and incoherent frequencies (red region) in the bunch as a function of intensity parameter, calculated using the Hofmann-Pedersen approach for $\eta > 0$ (LHC), $\mu = 0.5$ and $\tau = 1.05$ ns.

For short bunches in a stationary bucket, the LLD threshold can be presented in a simple form [13]

$$I_{\mathrm{th}} = F \frac{V h^3 (f_0 \tau)^5}{\mathrm{Im}Z/n} \qquad (8)$$

with the form-factor $F = \pi^4/30$. It agrees quite well ($\sim 30\%$ higher) with Sacherer criterion for dipole motion and $\mu = 0.5$, where $[\delta\omega_c/\Delta\omega_s]_{\mathrm{stab}} = 2/3$, giving $F = \pi^2/4$ in Eq. (8). As can be seen from Fig. 3, the threshold is much lower for $\eta \mathrm{Im}Z < 0$. This is the case for $\mu = 0.5$ only, for higher μ values, the situation can be opposite. The solutions for other particle distributions can be found in semi-analytical way using formula (7) and taking into account the potential well distortion for the calculation of both coherent (small effect) and incoherent synchrotron frequencies inside the bunch. The results of these calculations for bunch lengths, scaled from FWHM (full-width half-maximum) value found for each distribution for a Gaussian bunch, are shown in Fig. 4, with $\mu = 2$ suitable for the LHC bunch profiles [7].

As can be seen in Fig. 4, a large difference (almost factor 4) between measurements and predictions for a rigid-bunch dipole motion cannot be explained by a difference in particle

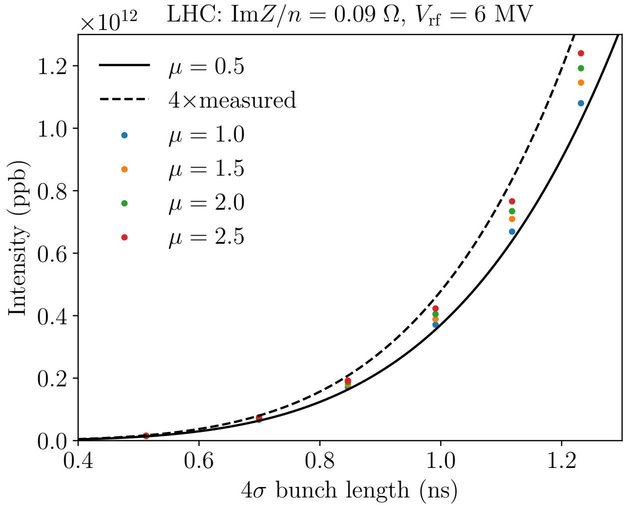

Figure 4: Intensity thresholds for the loss of Landau damping (LHC flat bottom energy of 0.45 TeV) as a function of bunch length (scaled from FWHM), calculated using the Hofmann-Pedersen approach for different particle distributions from binomial family (solid line for $\mu = 0.5$ and colored circles for $\mu - 1.0, 1.5, 2.0, 2.5$) together with the measured threshold (dashed black line) increased for comparison by a factor of 4.

distribution: the thresholds for various distributions are similar for the same FWHM bunch length (this was also seen in simulations [7]).

The Hofmann-Pedersen approach allows to find solutions for a rigid bunch motion in self-consistent way and it was also used for calculations of the LLD thresholds in single and double RF systems [14], [15].

VAN-KAMPEN MODES

There are several ways to find general solutions of the linearised Vlasov equation in the longitudinal plane for high azimuthal and radial modes without neglecting the synchrotron frequency spread [16] - [18], which allow then to obtain the LLD thresholds in a self-consistent way.

The method applied in Ref. [19] is based on appearance of so-called Van-Kampen modes [20] in solutions of the Vlasov equation for a perturbation $\tilde{\mathcal{F}}(\mathcal{E}, \psi, t)$ to a stationary distribution function $\mathcal{F}(\mathcal{E})$, expanded in harmonics m of synchrotron motion with eigen-functions $C_m(\mathcal{E})$ and $S_m(\mathcal{E})$ [18]:

$$\tilde{\mathcal{F}}(\mathcal{E}, \psi, t) = e^{-i\Omega t} \sum_{m=1}^{\infty} \left[C_m(\mathcal{E}) \cos m\psi + S_m(\mathcal{E}) \sin m\psi \right].$$

Substitution into the linearised Vlasov equation gives

$$\left[\Omega^2 - m^2 \omega_s^2(\mathcal{E})\right] C_m(\mathcal{E}) = -\frac{2i\, I_0 h\, m^2}{V \cos\phi_s} \omega_s^2(\mathcal{E}) \mathcal{F}'(\mathcal{E})$$

$$\times \sum_{m'=1}^{+\infty} \int_0^{\mathcal{E}_{\max}} \frac{d\mathcal{E}'}{\omega_s(\mathcal{E}')} \sum_{k=-\infty}^{+\infty} \frac{Z_k(\Omega)}{k} I_{mk}(\mathcal{E}) I^*_{m'k}(\mathcal{E}') C_{m'}(\mathcal{E}'),$$

where function

$$I_{mk}(\mathcal{E}) = \frac{1}{2\pi}\int_{-\pi}^{\pi} d\psi\, e^{i\frac{k}{h}\phi(\mathcal{E},\psi)-im\psi}, \tag{9}$$

and I_0 is the average beam current. When the integration over energy is replaced here by a sum, one has to solve an eigenvalue problem for the corresponding matrix equation. This technique was used to analyse numerically in Refs. [18], [21] - [23] bunch instability due to radial mode coupling and in Ref. [19] - the thresholds for the loss of Landau damping. Below the LLD threshold, there is a continuous spectrum consisting of singular modes from incoherent synchrotron frequency band. Existence of discrete modes, coherent solutions described by regular eigen-functions, outside incoherent band serves as a criterion for the LLD [17], [19]. This method was fruitfully applied to understand and cure dancing bunches at Tevatron [24]. The results of calculations for LHC are shown in Fig. 5. They agree with available experimetal data and simulations. However, as it was noticed already before [19], the LLD threshold from Van Kampen modes differs significantly from the Sacherer criterion.

The Van Kampen modes were used to compare the LLD thresholds in single and double RF systems [19], [25], [26].

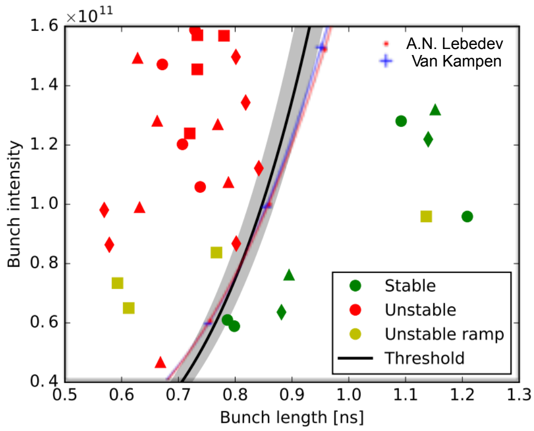

Figure 5: Measured (symbols) and calculated (red and blue lines) intensity thresholds versus bunch length in LHC (flat top energy 6.5 TeV, $V = 12$ MV) for the particle distribution (3) with $\mu = 2$.

LEBEDEV EQUATION

The first self-consistent system of equations suitable for analysis of beam stability thresholds was proposed by A. N. Lebedev in 1968 [16] and it can be written in the form (see also [27], [28])

$$\tilde{\lambda}_p(\Omega) = \frac{I_0 h}{V\cos\phi_s}\sum_{k=-\infty}^{\infty} G_{pk}(\Omega)\frac{Z_k(\Omega)}{k}\tilde{\lambda}_k(\Omega), \tag{10}$$

where the matrix elements are

$$G_{pk}(\Omega) = -2\pi i\,\omega_{s0}^2 \sum_{m=-\infty}^{\infty} m \times \int_0^{\mathcal{E}_{\max}} \frac{I_{mk}(\mathcal{E})I_{mp}^*(\mathcal{E})}{\Omega - m\omega_s(\mathcal{E})}\mathcal{F}'(\mathcal{E})\,d\mathcal{E},$$

and λ_k is Fourier harmonic of the line density perturbation. For short bunches in a single RF system $\phi(\mathcal{E},\psi) \simeq \sqrt{2\mathcal{E}}\cos\psi$, and function (9) can be presented as

$$I_{mk}(\mathcal{E}) \approx i^m J_m\left(\frac{k}{h}\sqrt{2\mathcal{E}}\right), \tag{11}$$

where $J_m(x)$ is the Bessel function of the first kind and the order m.

Matrix equation (10), converted into integral equation by performing inverse Fourier transform over azimuthal harmonics, was used for analysis of single-bunch stability threshold in presence of an inductive impedance with constant $\mathrm{Im}Z/n$ [16] and later in Ref. [29], where the threshold, very similar to the Sacherer criterion (6), was obtained.

For small arguments $k\sqrt{2\mathcal{E}}/h < 1$ in Eq.(11), or for the frequency range well inside stable bunch spectrum $f = kf_0 < 1/(\pi\tau)$, the Bessel function can be approximated as

$$J_m(k\sqrt{2\mathcal{E}}) \simeq \left(\frac{k}{h}\sqrt{2\mathcal{E}}\right)^m \frac{1}{2^m\, m!}. \tag{12}$$

In this case, for uncoupled mode m, the eigen-functions of Eq.(10) have a form

$$\lambda_k(\Omega) = \left(\frac{k}{h}\right)^m B_m(\Omega),$$

Using this solution in Eq.(10) and keeping only resonant term with positive m allows the dispersion relation (5) to be reproduced up to the coefficient in front of the integral, obtained here in the low-frequency approximation

$$1 = -\frac{i2\pi\omega_{s0}^2 I_0 h}{V\cos\phi_s}\,\frac{m}{2^m\,(m!)^2}\,Z_{\text{eff}}^* \times \int_0^{\infty}\frac{\mathcal{E}^m\mathcal{F}'(\mathcal{E})}{\Omega - m\omega_s(\mathcal{E})}d\mathcal{E}. \tag{13}$$

Here the effective impedance is defined as

$$Z_{\text{eff}}^* = \sum_{k=-\infty}^{\infty}\frac{Z_k}{k}\left(\frac{k}{h}\right)^{2m},$$

and it obviously doesn't converge for constant $\mathrm{Im}Z/k$ and, as Eq. (13) itself, is valid only for $k < 1/(\pi f_0\tau)$. So the Sacherer dispersion relation is applicable only in this, low-frequency approximation.

The matrix equation (10) has been solved numerically using the code MELODY [30] and the results for the LLD agree very well with those obtained from Van Kampen modes (see Fig. 5) for the same impedance model. However there is no threshold for a constant $\mathrm{Im}Z/n$ (the solution does not converge with higher and higher frequencies included), and the physical impedance model should be used. For LHC, the results strongly depend on the cut-off frequency $f_{\rm cut}$ for constant ImZ/n or the resonant frequency of the broad-band impedance model. Good agreement with measurements in LHC was obtained for $\mu = 2$ and broad-band impedance with $f_r = 5$ GHz, $Q = 1$, Im$Z/n = 0.076$ Ohm and $f_{\rm cut} = 20$ GHz. It is also observed that the potential well distortion does not affect the thresholds significantly.

DOUBLE RF SYSTEM

The most efficient way to increase synchrotron frequency spread inside the bunch is to use a higher harmonic RF system. The total RF voltage will be

$$V_t = V_1 \sin\phi + V_2 \sin(n\phi + \phi_2),$$

where the phase ϕ_2 defines the mode of operation: bunch-lengthening (BL) if total voltage gradient at bunch center is reduced and bunch-shortening (BS), if increased. At CERN, a higher harmonic RF system is applied for beam stabilisation in the SPS (with $n = 4$) [31]; it was considered for LHC (with $n = 2$) [7] and for the PS (with $n = 3 - 4$) [32].

Only the BS-mode is used at CERN for beam stabilisation, since the application of the BL-mode for multi-bunch beams is less obvious [31]. One of the main reasons is an existence of the flat region in the synchrotron frequency distribution ($\omega_s'(\mathcal{E}) \sim 0$) inside the bunch, where $\mathcal{F}'(\mathcal{E}) \neq 0$ [33]. This problem can be seen from Eq.(10), where, at the threshold of stability, the element G_{pk} can be written in the form

$$G_{pk}(\Omega) = -2\pi^2\,\mathrm{sgn}(\Omega) \sum_{m=1}^{\infty} \frac{\omega_{s0}^2\,\mathcal{F}'(\mathcal{E}_m)}{\omega_s'(\mathcal{E}_m)} I_{mk}(\mathcal{E}_m) I_{mp}^*(\mathcal{E}_m)$$

$$-i\,4\pi\omega_{s0}^2 \sum_{m=1}^{\infty} \mathcal{P}\int_0^{\mathcal{E}_{\max}} d\mathcal{E}\,\mathcal{F}'(\mathcal{E}) \frac{I_{mk}(\mathcal{E}) I_{mp}^*(\mathcal{E})\,\omega_s(\mathcal{E})}{\Omega^2/m^2 - \omega_s^2(\mathcal{E})}.$$

Here $\mathcal{E}_m$ is defined by $|\Omega| = m\omega_s(\mathcal{E}_m)$ if the coherent mode frequency belongs to the incoherent frequency band, and $\mathcal{P}$ denotes the principle value.

Equation (10) becomes very simple when used for a narrow-band impedance with resonant frequency f_r, so that only azimuthal harmonics with $k \sim f_r/f_0$ can be kept. The stability threshold of a multi-bunch beam in a double RF system is not defined if the region with $\omega_s'(\mathcal{E}) \sim 0$ is inside bunch emittance [33].

A similar region, with $\omega_s'(\mathcal{E}) \sim 0$, may also exist in the BS-mode for $n > 2$ above certain voltage ratio V_2/V_1, see Fig. 6. However, for the same voltage V_2, the relative synchrotron frequency spread increases with n, and therefore large n is still attractive as a design choice if used for relatively short bunches.

Possible reduction of stability threshold for large bunch emittances in both BS-mode and BL-mode was confirmed in simulations [19], [25], [26], see also example in Fig. 7. In simulations, in order to excite the coherent motion of the particles, a small phase kick is initially given to the matched bunch. The LLD threshold is then determined from the residual bunch oscillations and in particular, by the ratio of the residual maximum amplitude oscillations to the initial kick. However, special care should be taken when defining this threshold, since it may strongly depend on the criterion chosen. This is illustrated in Fig. 7, where the residual oscillation amplitude found from simulations for a double RF system (BL-mode) is shown [26]. As can be seen in the plot, a selection of a certain criterion (horizontal line in the plot) affects the absolute LLD threshold, although it gives similar relative results (for the different emittances).

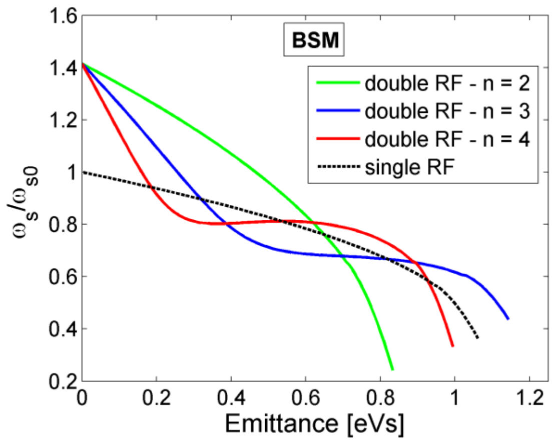

Figure 6: Relative synchrotron frequency as a function of longitudinal emittance in double RF system in BS-mode with different n and $V_1/V_2 = n$ (example for the SPS bottom energy).

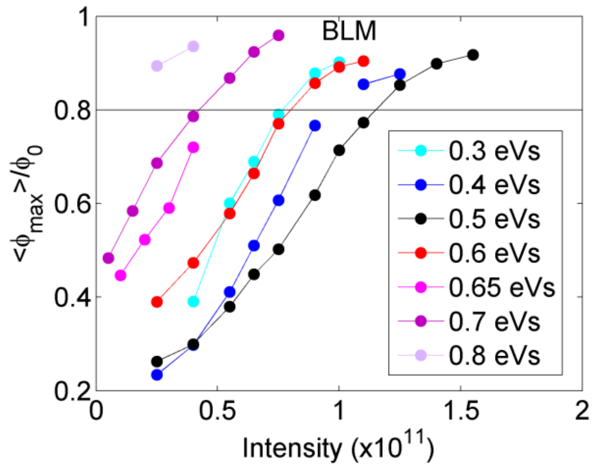

Figure 7: Ratio of the residual dipole oscillation amplitude to the amplitude of the initial phase kick (color circles) as a function of the bunch intensity found in simulations performed for various bunch emittances in a double RF system with $n = 2$ (BL-mode). The horizontal line indicates a possible criterion for the LLD threshold.

SUMMARY

In longitudinal plane, simplified analytical criteria are often used for the scaling of the loss of Landau damping threshold with beam and machine parameters. The Sacherer stability diagram in longitudinal plane is justified only for low-frequency impedance and in other cases should be used with caution. More advanced methods (Van-Kampen modes and Lebedev equation) together with particle simulations are available for accurate threshold estimations, also based on a realistic impedance model, since a constant $\mathrm{Im}Z/n$ may not give converging LLD thresholds. In case of $\eta \mathrm{Im}Z/n > 0$, the dependence of thresholds on particle distribution can be reduced by using the FWHM bunch lengths.

Landau damping can be significantly increased by additional, higher harmonic RF system, but its limitations in BL-mode and, for $n > 2$, in BS-mode should be taken into account for the choice of the beam and RF parameters.

ACKNOWLEDGMENTS

We acknowledge important input from J. E. Muller and useful discussion with A. Burov.

REFERENCES

[1] The LHC Study Group, "The Large Hadron Collider - Conceptual Design", CERN/AC/95-05 (LHC) (1995).

[2] F. Sacherer, Methods for computing bunched beam instabilities, CERN/SI-BR/72-5 (1972).

[3] F. Sacherer, A longitudinal stability criterion for bunched beams, IEEE Transactions on Nuclear Science, 825-829, (1973).

[4] K. Hubner and V.G. Vaccaro, Dispersion relations and stability of coasting beams, CERN-ISR-TH/70-44 (1970).

[5] D. Boussard, D. Brandt and L. Vos, Is a longitudinal feedback required for LHC? CERN LHC-Project-Note-205 (1999).

[6] E. Shaposhnikova, Longitudinal beam parameters during acceleration in the LHC, CERN LHC-Project-Note-242 (2000).

[7] J. Esteban Muller, Longitudinal intensity effects in the CERN Large Hadron Collider, PhD thesis, Apr 2016, `https://cds.cern.ch/record/2196930`.

[8] BLonD: Beam Longitudinal Dynamics code, CERN website `http://blond.web.cern.ch`.

[9] N. Mounet, The LHC transverse coupled-bunch instability. PhD thesis, EPFL (2012).

[10] E. Metral, Longitudinal bunched-beam coherent modes: from stability to instability and inversely, CERN-AB-2004-002 ABP (2004).

[11] K.Y. Ng, Physics of Intensity Dependent Beam Instabilities, World Scientific Publishing (2006).

[12] I.S. Gonzalez, Loss of longitudinal Landau damping in the LHC injectors, CERN AB-Note-2008-001 ABP (2008).

[13] A. Hofmann and F. Pedersen. Bunches with local elliptic energy distributions. IEEE Transactions on Nuclear Science, 26(3):3526–3528 (1979).

[14] O. Boine-Frankenheim and T. Shukla, Space charge effects in bunches for different rf wave forms, PRST-AB **8**, 034201 (2005).

[15] O. Boine-Frankenheim and O. Chorniy, Stability of coherent synchrotron oscillations with space charge, PRST-AB **10**, 104202 (2007).

[16] A.N. Lebedev, Coherent synchrotron oscillations in the presence of a space charge, Sov. Atom. Energy. vol. 25, n0. 2, pp.851-856 (1968).

[17] Y.H. Chin, K. Satoh and K. Yokoya, Instability of a bunched beam with synchrotron frequency spread, PA 13 (1983) 45.

[18] Oide and Yokoya, Longitudinal single bunch instability in electron storage rings, KEK Preprint 90-10 (1990).

[19] A. Burov, Van Kampen modes for bunch longitudinal motion, 46th ICFA Advanced Beam Dynamics Workshop HB2010, Morschach, Switzerland (2010).

[20] N. G. van Kampen. The dispersion equation for plasma waves. Physica, 23:641–650, (1957).

[21] M. D'yachkov and R. Baartman, Longitudinal single bunch stability, Part. Acc. 50, 105 (1995).

[22] K. Oide, A mechanism of longitudinal single-bunch instability in storage rings, Part. Acc, 51, 43 (1995).

[23] A. Mosnier, Microwave instability in electron storage rings, Nucl. Instrum. Methods Phys. Res., Sect. A 438, 225 (1999).

[24] A. Burov, Dancing bunches as Van Kampen modes, FERMILAB-CONF-1-121-AD (2011).

[25] T. Argyropoulos, A. Burov, E. Shaposhnikova, Loss of Landau damping for inductive impedance in a double RF system, IPAC'13 (2013).

[26] T. Argyropoulos, Longitudinal beam instabilities in a double RF system, PhD thesis CERN-THESIS-2015-421 (2015).

[27] V.I. Balbekov, S.V. Ivanov, Longitudinal instability threshold of bunched beams in proton synchrotrons, Sov. Atom. Energy, vol.60, no. 1, pp.58-66 (1986).

[28] E. Shaposhnikova, Bunched beam transfer matrices in single and double RF systems. Tech. Rep. CERN-SL-94-19-RF (1994).

[29] V.I. Balbekov and S.V. Ivanov, Thresholds of longitudinal instability of bunched beam in the presence of dominant inductive impedance. IHEP Preprint 91-14, Protvino (1991).

[30] I. Karpov, Matrix Equations for LOngitudinal beam DYnamics (MELODY) code, `https://gitlab.cern.ch/ikarpov/melody`.

[31] E. Shaposhnikova, T. Bohl, and T.P.R. Linnecar, Beam transfer functions and beam stabilisation in a double RF system, CERN-AB-2005-026 (2005).

[32] H. Damerau, A. Lasheen, E. Shaposhnikova, Higher-harmonic RF system for Landau damping in the CERN PS, IPAC'18 (2018).

[33] S.V. Ivanov and V.I. Balbekov, Methods for suppressing the longitudinal instability of a bunched beam with the help of Landau damping. Atom. Energ., 62 (2) pp.117–125 (1987).